Electronic Supplementary Information

for

Single-crystal-to-single-crystal synthesis of a pseudostarch via topochemical azide-alkyne cycloaddition polymerization

Arthi Ravi, Amina Shijad, and Kana M. Sureshan*

1. Experimental procedures

All chemicals were purchased from Sigma Aldrich and Spectrochem and used without further purification. All solvents were purchased from Merck and distilled before use. Thin layer chromatography was carried out using pre-coated silica gel 60 F254 (Merck) plates. The thin layer chromatograms were visualized by dipping the plates into a solution of ceric ammonium molybdate stain, followed by heating with a hot air gun. Flash column chromatography was carried out in silica gel (200-400 mesh). NMR spectra were recorded in a Avance III-500 (Bruker) NMR spectrometer. The ^{1}H NMR spectra were recorded at 500 MHz and the ^{13}C NMR spectra were proton decoupled and recorded at 125 MHz. All signals were assigned on the basis of ^{1}H, ^{13}C, COSY, DEPT, HMQC and HMBC spectra. The chemical shifts of the proton (δ) and carbon signals are reported in ppm with reference to the internal standard tetramethylsilane (TMS, $\delta = 0.0$ ppm) or with the solvent reference relative to TMS. ESI-HRMS mass spectra were recorded using orbitrap mass spectrometer (Thermo Exactive). MALDI analysis was carried out in a Bruker UltrafleXtreme MALDI-TOF Mass Spectrometer. The matrix used was dihydroxy benzoic acid. The samples were dissolved in suitable solvents and then mixed with a solution of the matrix in TA 30. The mixture was spotted on the ground-steel plate and allowed to dry at room temperature. IR spectra were recorded on an IR Prestige-21 instrument using the KBr pellet method. Melting points were recorded on a Stuart SMP 30 melting point apparatus. Single crystal X-ray intensity data were collected on a Bruker KAPPA APEX-II diffractometer in omega and phi scan mode, MoKα = 0.71073 Å. Refinement was carried out with SHELXL-2014.[1,2] Powder X-ray diffraction analysis was carried out on a X'pert PRO (PANalytics) diffractometer. DSC thermograms were recorded on DSC Q20 Differential Scanning Calorimeter. Thermogravimetric analysis (TGA) was carried out on a Universal V4.7A TA instrument. Optical microscope images were recorded with a Qimaging Qclick camera mounted on Olympus BX51 microscope. The dimensions of the crystals were measured using the Qimaging QCapture Pro 7 software. GPC analysis was performed on Agilent 1260 Infinity GPC/SEC MDS system using DMSO as eluent. A mixture of pullulan polysaccharides (M_p: 667-642000 g/mol) was used as a standard. CHNS analysis were carried out in a Vario MICRO Cube Elementar CHNS Analyzer.

2. Origin of the design

The crystal structures of several cyclitols and pyranoses with trans vicinal-diequatorial diols are reported in literature. The crystal structures of diols A-O (Chart S1) showed a 1D zigzag hydrogen bonding.

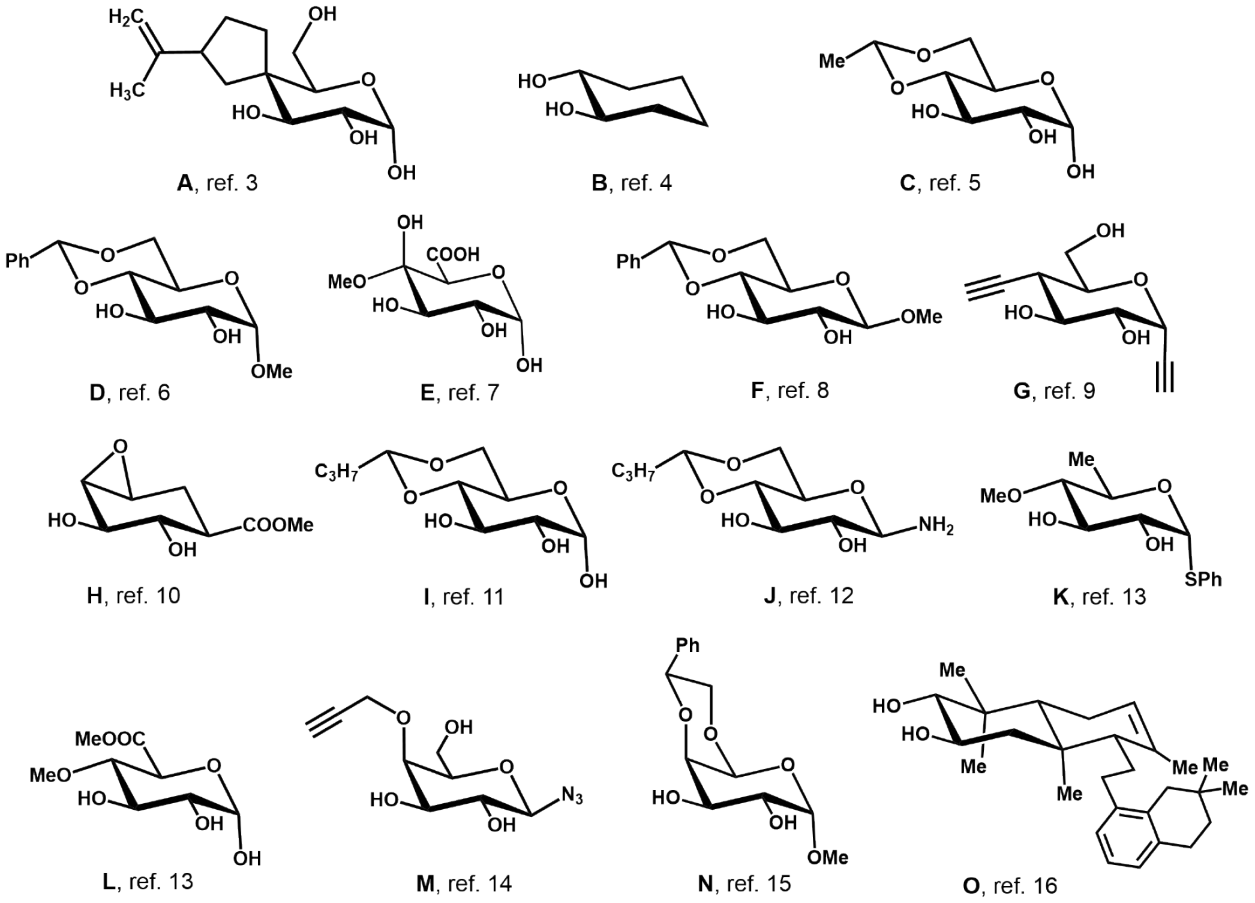

Chart S1. Chemical structures of pyranoses and cyclitols containing vicinal-diequatorial diol units, whose crystal structures show a conserved packing with zigzag 1D-hydrogen bonded assembly.

3. Synthesis and characterization of monomer 1 (5-azido-2-*O*-propargyl-*myo*-inositol)

Compound **8** was synthesized using the procedure reported by Ravi *et al*.[17] To compound **8** (502 mg, 1.07 mmol), 5 mL of 9:1/TFA:H_2O was added and the reaction mixture was allowed to stir for 15 minutes. The reaction mixture turned yellow, and TLC showed complete consumption of the starting material. The above mixture was concentrated under reduced pressure. The resulting residue was washed with ethyl acetate and dried under vacuum, yielding monomer **1** as a white solid (258 mg, quant.). Crystals of monomer **1** were obtained by slow evaporation from a saturated solution of the compound in acetonitrile kept at 28 °C. ^{1}H NMR (500 MHz, DMSO-d_6) δ_H 5.21 (d, J = 5 Hz, 2H, O*H*), 4.84 (d, J = 5 Hz, 2H, O*H*), 4.37 (d, J = 2.5 Hz, 2H, CH_2), 3.67 (1H, H-2), 3.32 (5H, H-1, H-3, C≡C-*H*, H-4 & H-6), 2.99 (t, J = 9 Hz, 1H, H-5); ^{13}C NMR (125 MHz, DMSO-d_6) δ_C 86.42 (*C*≡C-H), 85.56 (C-2), 81.69 (C≡*C*-H), 77.25 (C-4, C-6), 76.58 (C-1, C-3), 74.36 (C-5), 64.74 (*C*H_2); IR (KBr): 3321 cm^{-1} (-OH), 3289 cm^{-1} (C≡C), 2110 cm^{-1} (azide). Mass Calculated m/z = 243.08; Found m/z = 266.30 $(M+Na)^+$. The compound melted at 317 °C. CHNS analysis: Calculated for $C_9H_{13}N_3O_5$: C = 44.44, H = 5.39, N = 17.28; Found: C = 44.36, H = 5.34, N = 17.33.

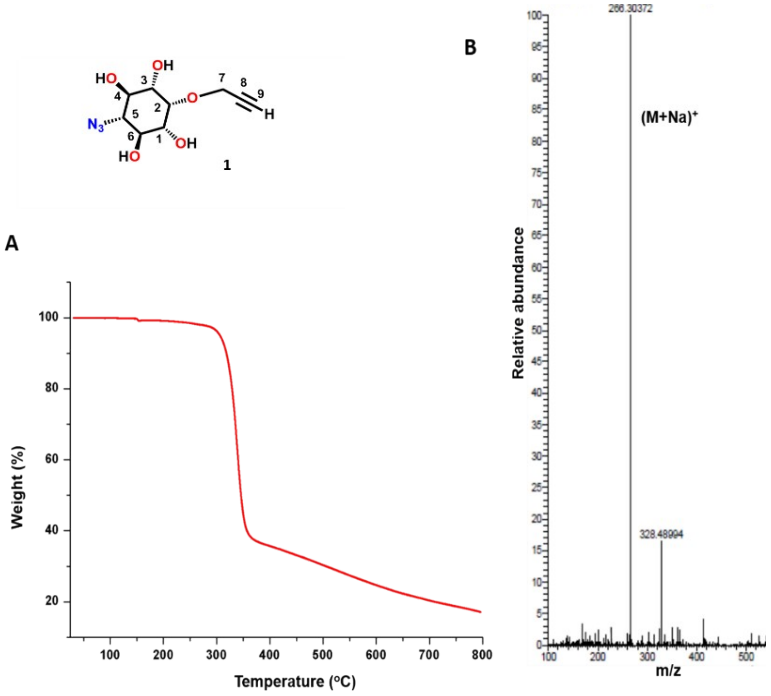

Figure S1. A) TGA analysis of monomer **1**; heating rate was maintained at 5 °C/min. B) HRMS analysis of monomer **1**.

4. Crystal data

Table S1. Crystal data for monomer **1** and polymer **2**.

Data	Monomer **1**	Polymer **2**
Formula	$C_9H_{13}N_3O_5$	$C_9H_{13}N_3O_5$
CCDC deposition numbers	CCDC 2038869	CCDC 2038870
Temperature	296(2) K	293(2) K
Wavelength	0.71073 Å	0.71073 Å
Crystal system, space group	Monoclinic, $P2_1/n$	Monoclinic, $P2_1/c$
Unit cell dimensions	a = 6.6496(5) Å b = 18.782(2) Å c = 9.0830(8) Å α = 90° β= 105.116(5)° γ = 90°	a = 6.792(2) Å b = 17.062(5) Å c = 9.698(3) Å α = 90° β = 109.159(8)° γ = 90°
Volume	1095.14(17) Å^3	1061.5(6) Å^3
Z	4	4
Density	1.475 g/cm^3	1.522 g/cm^3
Absorption coefficient	0.122 mm^{-1}	0.125 mm^{-1}
F (000)	512	512
Crystal size	0.250 x 0.150 x 0.020 mm^3	0.250 x 0.120 x 0.050 mm^3
Theta range for data collection	2.169 to 24.993°	2.523 to 24.993°
Reflections collected	20163	14418
Index ranges	-7<=h<=7 -10<=k<=22 -10<=l<=10	-8<=h<=8 -20<=k<=20 -11<=l<=11
Independent reflections	1920 [R(int) = 0.0220]	1868 [R(int) = 0.0810]
Completeness to theta = 25.242°	97.6 %	99.9 %
Absorption correction	Semi-empirical from equivalents	Semi-empirical from equivalents
Max. and min. transmission	0.9976 and 0.9702	0.994 and 0.969
Refinement method	Full-matrix least-squares on F^2	Full-matrix least-squares on F^2
Data / restraints / parameters	1920 / 1 / 158	1868 / 0 / 158
Goodness-of-fit on F^2	1.056	1.047

Final R indices [I>2sigma(I)]	R1 = 0.0337, wR2 = 0.0755	R1 = 0.0496, wR2 = 0.1168
R indices (all data)	R1 = 0.0483, wR2 = 0.0841	R1 = 0.0885, wR2 = 0.1363
Largest diff. peak and hole	0.222 and -0.168 e.Å^{-3}	0.486 and -0.305 e.Å^{-3}

Table S2. List of hydrogen bonds in crystals of monomer **1** and polymer **2**.

Monomer **1**			Polymer **2**		
D-H…A	H…A (Å) / D-H…A (°)	Symmetry code	D-H…A	H…A (Å) / D-H…A (°)	Symmetry code
C-H…O hydrogen bonding					
C6-H6…O4	2.63 / 3.34 / 129.3	-½+x, 1.5-y, ½+z	C9-H9…O3	2.31 / 3.24 / 173.4	-1+x, 1.5-y, -½+z
C9-H9…O3	2.68 / 4.71 / 160.9	2-x, 1-y, 1-z			
O-H…O hydrogen bonding					
O3-H3A…O1	2.00 / 2.79 / 164.2	1+x, y, z	O3-H3A…O1	1.96 / 2.77 / 173	1+x, y, z
O4-H4A…O6	1.91 / 2.73 / 176.3	1+x, y, z	O4-H4A…O6	2.38 / 3.11 / 148.1	1+x, 1.5-y, ½+z
O1-H1A…O4	2.00 / 2.79 / 171.8	-½+x, 1.5-y, ½+z	O6-H6A…O4	2.02 / 2.84 / 172.7	-1+x, y, z
O6A-H6A…O3	2.04 / 2.8 / 154.2	-½+x, 1.5-y, ½+z			
C-H…N hydrogen bonding					
			C3-H3…N2	2.64 / 3.57 / 158.4	x, 1.5-y, -1/2+z
			C1-H1…N3	2.68 / 3.56 / 149.7	1-x, 1-y, -z
O-H…N hydrogen bonding					
			O1-H1A…N3	2.04 / 2.85 / 172.9	x, y, z

5. Topochemical polymerization of monomer 1

Single crystals of monomer **1** (500 mg) were taken in a glass vial and heated at 80 °C in an oil bath. Approximately 20 mg each of this sample was withdrawn at different times and used for analysis by time-dependent ^{1}H NMR, DSC, PXRD and IR techniques. ^{1}H NMR was recorded by dissolving the sample in DMSO-d_6. IR spectra was recorded by making a pellet with KBr. The crystals were crushed to powder and analyzed by PXRD.

The kinetics of the azide-alkyne cycloaddition reaction at 80 °C was studied by time-dependent ^{1}H NMR spectroscopy. The gradual disappearance of the signals due to the monomer **1** and the concomitant emergence of signals due to the corresponding polymer was observed with time. The ^{1}H NMR was recorded until no considerable change in the ratio of product formed was observed. A plot of percentage of reaction versus time suggested that the reaction follows sigmoidal kinetics, as expected for topochemical reactions (Figure S2). The -CH_2 proton signal at δ 4.38 and the triazolyl proton signals from δ 7.86-7.96 were integrated and the relative integration was used to calculate the percentage of conversion at each stage by the following equation.

$$\% \text{ of conversion} = \frac{(\text{Area of peaks in region } \delta\ 7.86\text{-}7.96) \times 100}{\left[\text{Area of peaks in region } \delta\ 7.86\text{-}7.96 + \frac{(\text{Area of peak at } \delta\ 4.38)}{2}\right]}$$

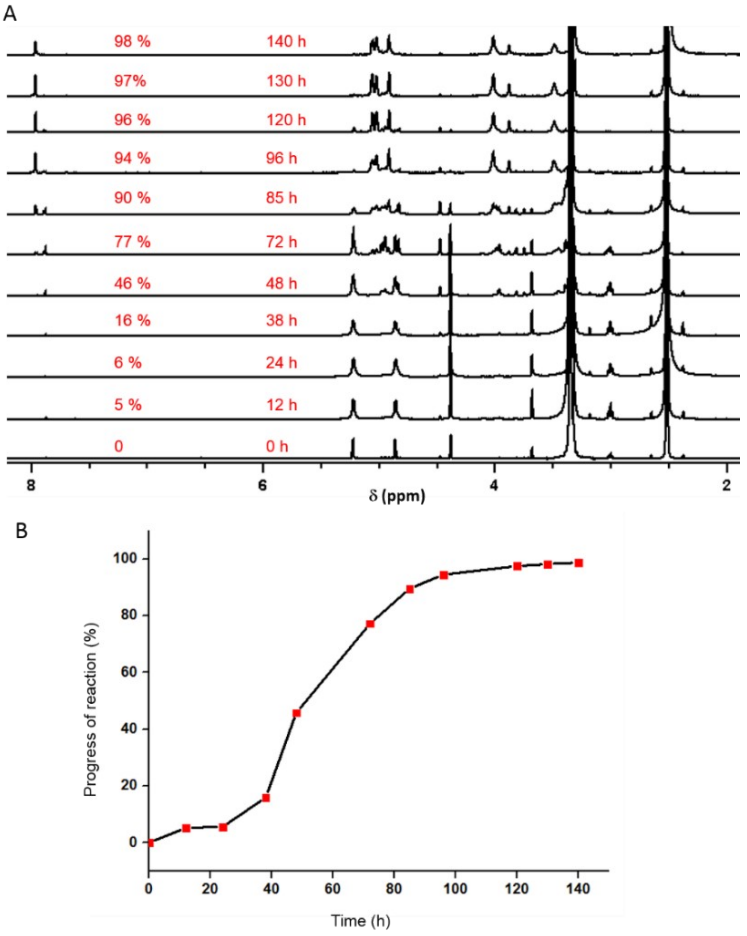

Figure S2. A) Time-dependent ^{1}H NMR spectra of monomer **1** at 80 °C. The spectra were recorded after dissolving monomer **1** in DMSO-d_6. B) Progress of azide-alkyne cycloaddition reaction of monomer **1** at 80 °C with time. The reaction follows sigmoidal kinetics.

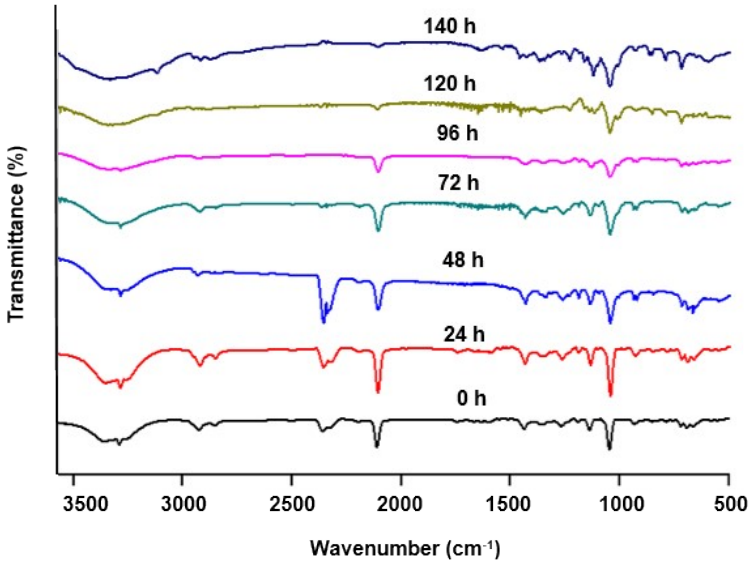

Figure S3. Time-dependant IR analyses of the monomer **1** heated at 80 °C.

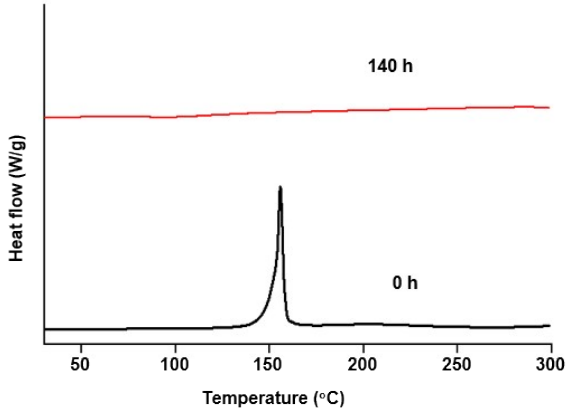

Figure S4. DSC thermograms of monomer **1** (0 h) and of monomer **1** heated at 80 °C for 140 h. The exothermic peak observed for the monomer **1** (0 h) is due to uncontrolled azide-alkyne cycloaddition of monomer **1**.

6. Characterization of polymer 2

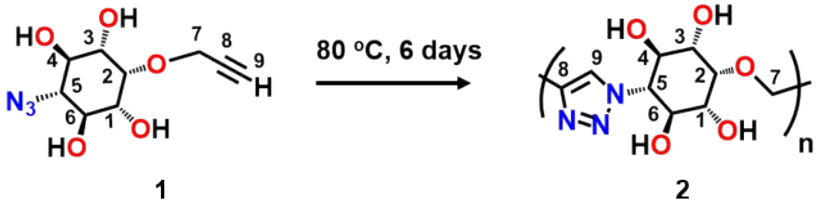

Scheme S1. Synthesis of polymer **2**.

Crystals of monomer **1** were heated in a glass vial for 140 h at 80 °C. ^{1}H NMR of the product showed the complete consumption of starting material. The resulting crystals were characterized using NMR, IR, MALDI-TOF-MS and SCXRD. ^{1}H NMR (500 MHz, DMSO-d$_6$): δ_H 7.96 (s, 1H, triazolyl-H), 5.06 (d, J = 4.75 Hz, 2H, OH), 5.02 (s, 2H, OH), 4.91 (s, 2H, CH_2), 4.01 (s, 3H, H-4, H-5 & H-6), 3.87 (s, 1H, H-2), 3.48 (s, 2H, H-1 & H-3); ^{13}C NMR (125 MHz, DMSO-d$_6$): δ_C 144.73 (*C*=C-H), 124.88 (C=*C*-H), 82.79 (C-2), 73.39 (C-1 & C-3), 71.42 (C-4 & C-6), 68.26 (C-5), 67.53 (CH_2). The MALDI-TOF mass spectrum showed presence of up to 43-mer. The polymer **2** was found to be stable up to 344 °C.

Assigning regiochemistry of the polymer 2

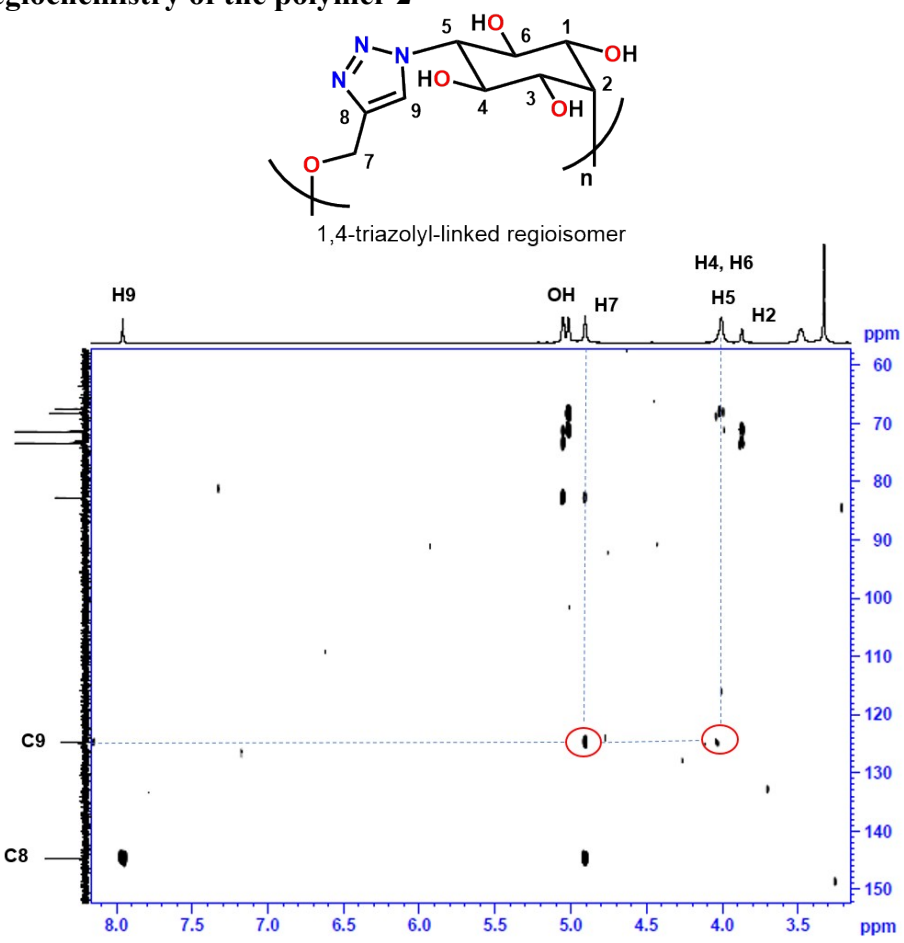

Figure S5. HMBC spectrum of the polymer **2** in DMSO-d$_6$.

The regiochemistry of the polymer **2** was determined from NMR spectra of the polymer taken after dissolution in DMSO-d$_6$. Triazolyl protons, due to the various oligomers formed, appeared as a singlet at δ_H 7.96. This suggests that the triazole linkages in all the oligomers are identical. This

linker homogeneity arises from the regiospecific cycloaddition reaction. HMBC spectrum of the polymer **2** shows the coupling of C9 with both H5 and H7, which is possible only in the 1,4-triazolyl regioisomer. Similarly, the NOESY spectrum shows that the triazolyl proton at H9 spatially interacts with both H7 and H5. This is possible only in the case of a 1,4-triazolyl linkage.

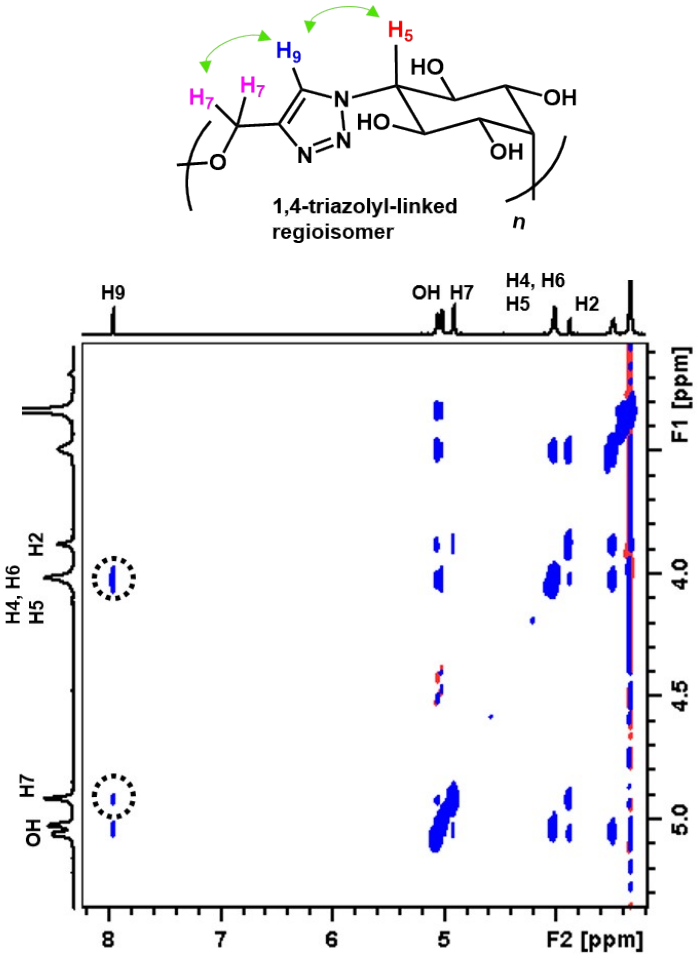

Figure S6. NOESY spectrum of the polymer **2** formed from TAAC reaction of monomer **1** recorded in DMSO-d_6, showing cross-peaks corresponding to 1,4-triazolyl linkage.

7. Solution-state studies

Huisgen reaction of monomer 1: 5 mg of monomer **1** was dissolved in 0.2 mL of DMSO. The solution was heated at 100℃ for 5 h. Then the mixture was lyophilized to remove the solvent and the products were analyzed by ^{1}H NMR. A mixture of triazole-linked products formed, as evident

from the newly formed triazole peaks at δ 7.95, 7.88 and 7.63. However, there was still unreacted starting material present.

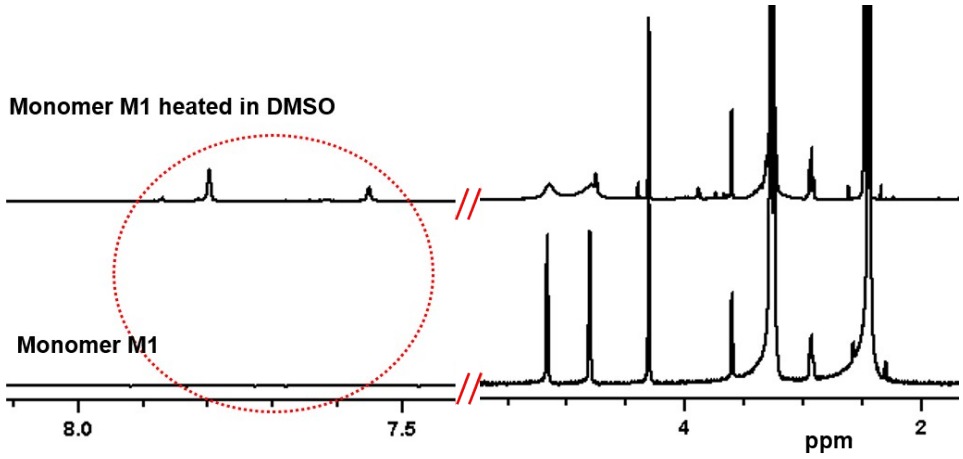

Figure S7. A comparison of the ^{1}H NMR spectra of monomer **1** and reaction mixture formed by heating monomer **1** dissolved in DMSO. The spectra were recorded in DMSO-d_6.

8. Features of monomer 1 and polymer 2 single crystals

Face-indexing of the monomer **1** was carried out using the Bruker KAPPA APEX-II diffractometer (APEX3). Bravais-Friedel-Donnay-Harker (BFDH) theoretical morphology was calculated using Mercury and the face-indices were matched (Figure S8). A comparison of the BFDH morphologies of the monomer **1** and the polymer **2** shows that the cycloaddition reaction occurs along '*b*' direction, but to achieve this the molecules must move closer to each other along '*b*' direction (height of the crystal). This accounts for the decrease in unit cell dimension along '*b*'-axis. To compensate for this change in volume, the unit cell dimensions increase along '*a*' and '*c*' directions.

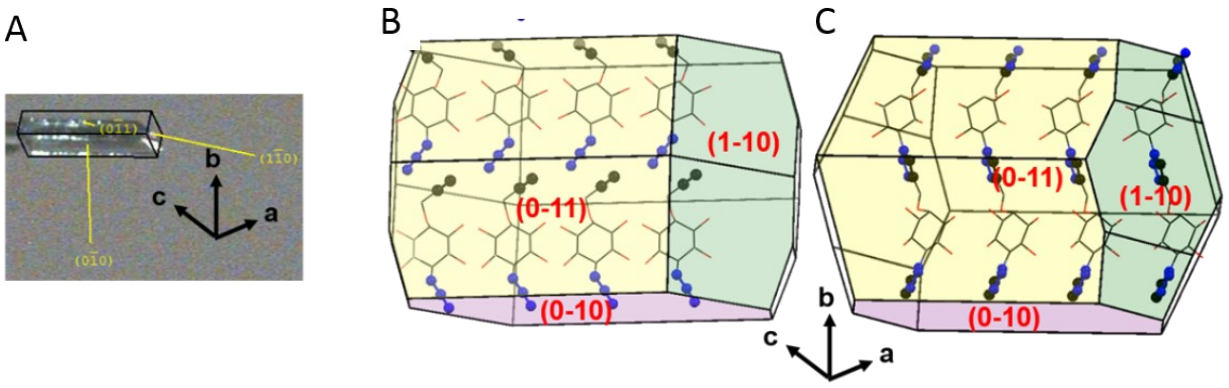

Figure S8. A) Face-indexing of crystal of monomer **1**. B) BFDH morphology of monomer **1**. C) BFDH morphology of polymer **2**.

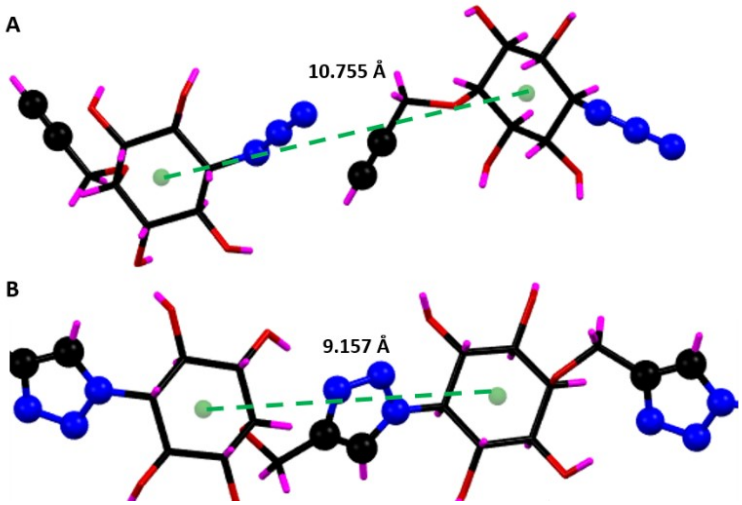

Figure S9. Distance between centroids of adjacent molecules in A) monomer **1** = 10.755 Å and B) polymer **2** = 9.157 Å.

9. MALDI-TOF-MS analyses of polymer 2

The polymer sample was dissolved in DMSO (1 mg in 10 µL) and diluted with TA30 solution (30 % acetonitrile and 70 % of 0.1 % TFA in water). 1 µL of the above solution was mixed with 1 µL of the DHB matrix solution (in TA30) and the mixture was spotted on the ground steel plate.

Results: Polymer **2**: Oligomers up to 43-mer were identified.

To determine the oligomers soluble in water, only the water-soluble fraction of the polymer samples was used for analysis. The results are given in Figure S10.

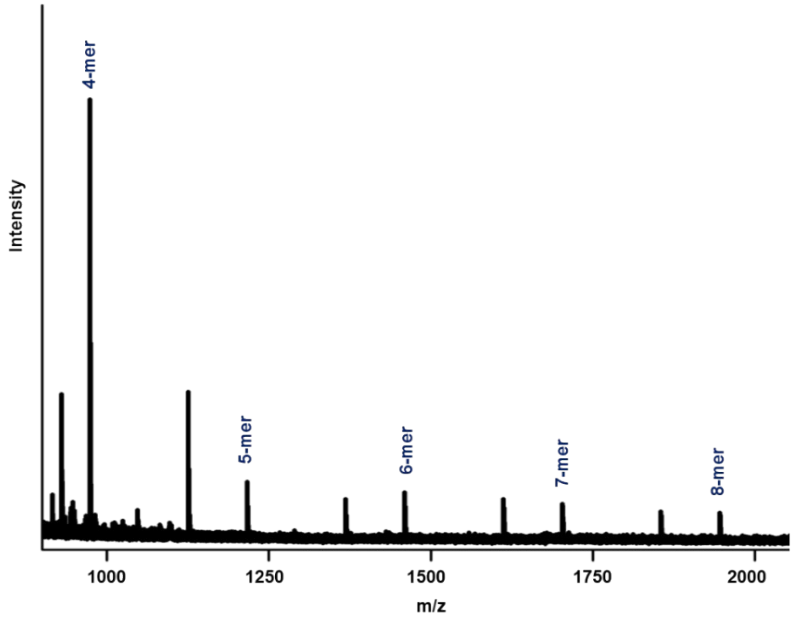

Figure S10. MALDI-TOF-MS analysis of the water-soluble fraction of polymer **2**.

10. GPC analyses

GPC analysis of the polymer **2** was carried out using a PLgel 10 µm Mixed B column using DMSO as eluent, at 50 °C with a flow rate of 0.2 mL/min. A mixture of pullulan polysaccharides (M_p = 667-642000 g/mol) dissolved in DMSO was used to generate a standard calibration curve and similar conditions were maintained. Conventional analysis by comparing the RI trace of polymers with standards was carried out. The results are as follows.

Polymer **2**: M_n = 4.9 kg/mol; M_w = 14.2 kg/mol; M_n/M_w = dispersity (Đ) = 2.9

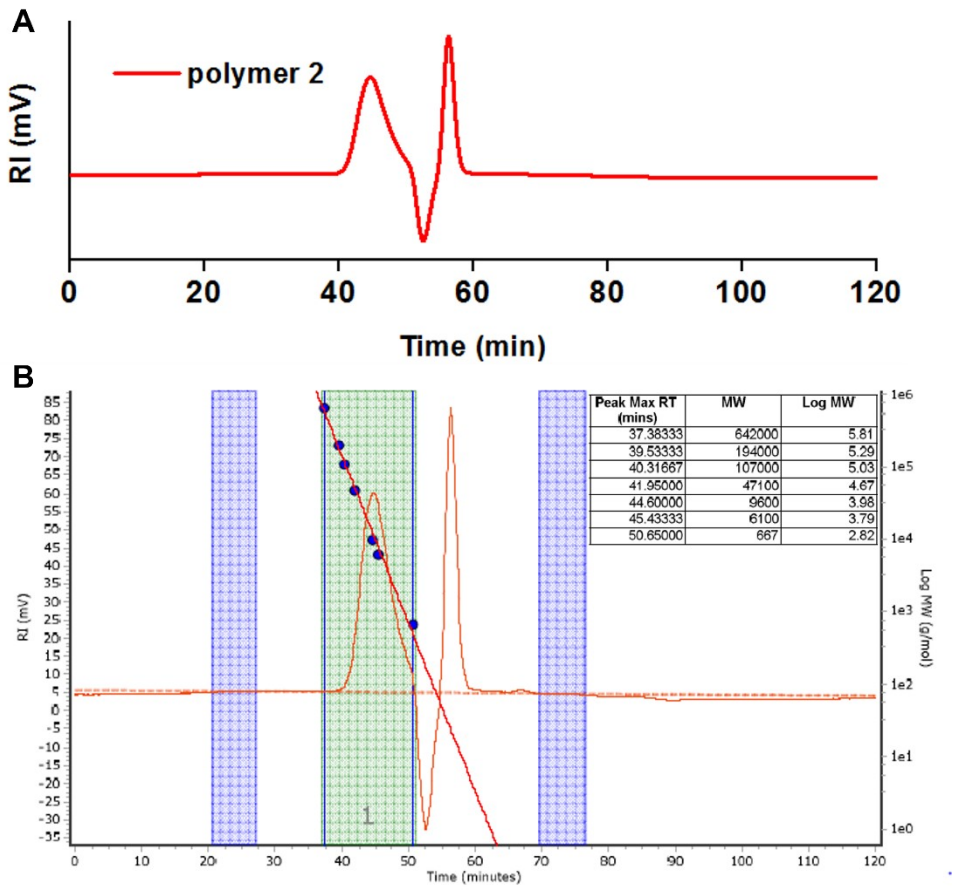

Figure S11. A) GPC elution curve of polymer **2**. B) RI trace of polymer **2** fitted to the standard calibration curve. The inset depicts the elution time and the molecular weights of the standard pullulan polysaccharides.

11. Amorphous thin film of polymer 2

The single crystals of polymer **2** were dissolved in DMSO (10 wt %) and poured on a petri dish. The solvent was allowed to evaporate at 70 ^{o}C for 15 days, resulting in thin films of the polymer. PXRD analysis of the thin film displayed broad peaks, indicating its amorphous nature.

12. Spectral data

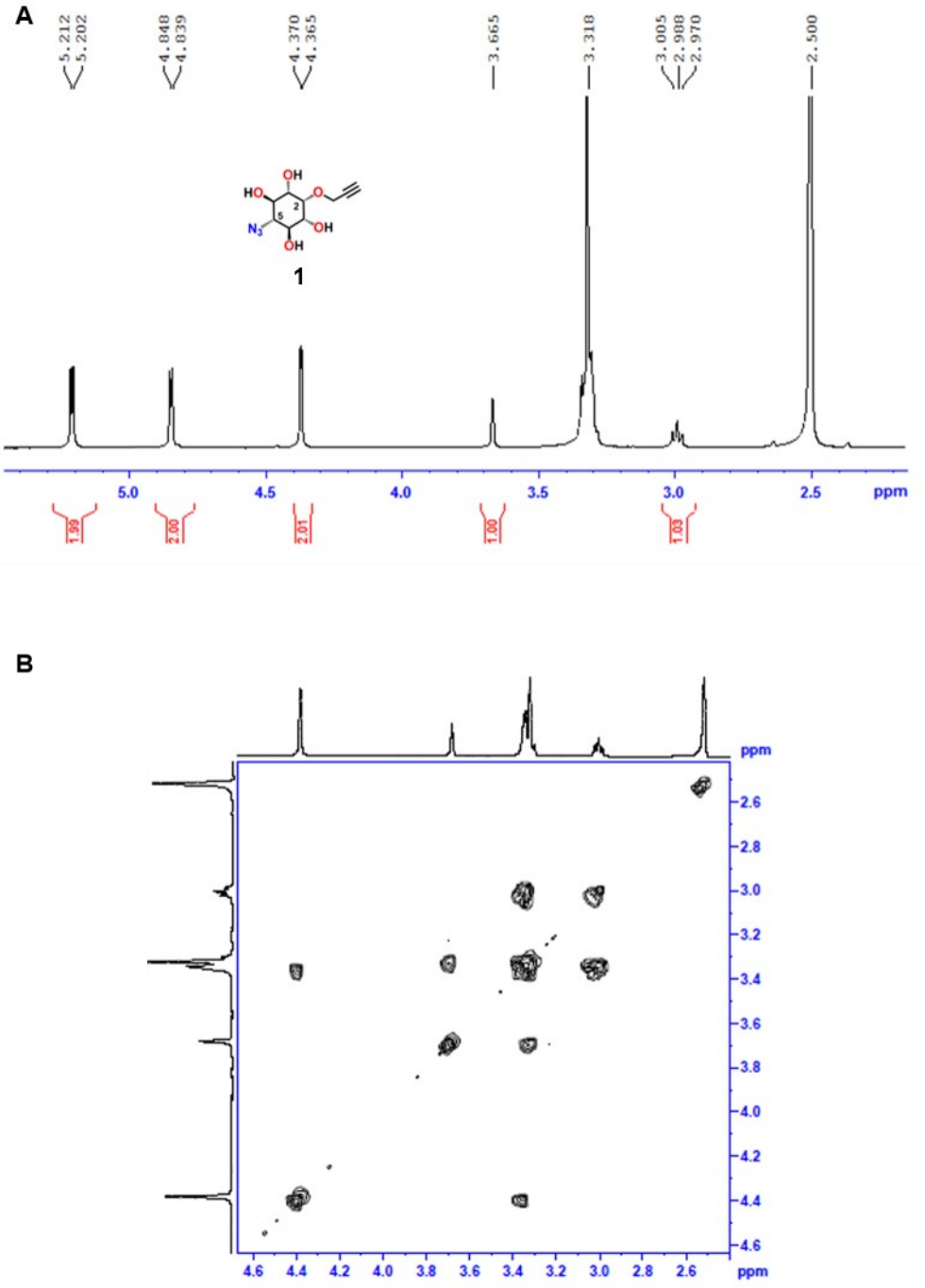

Figure S12. A) ^{1}H NMR and B) COSY spectra of monomer **1** in DMSO-d_6.

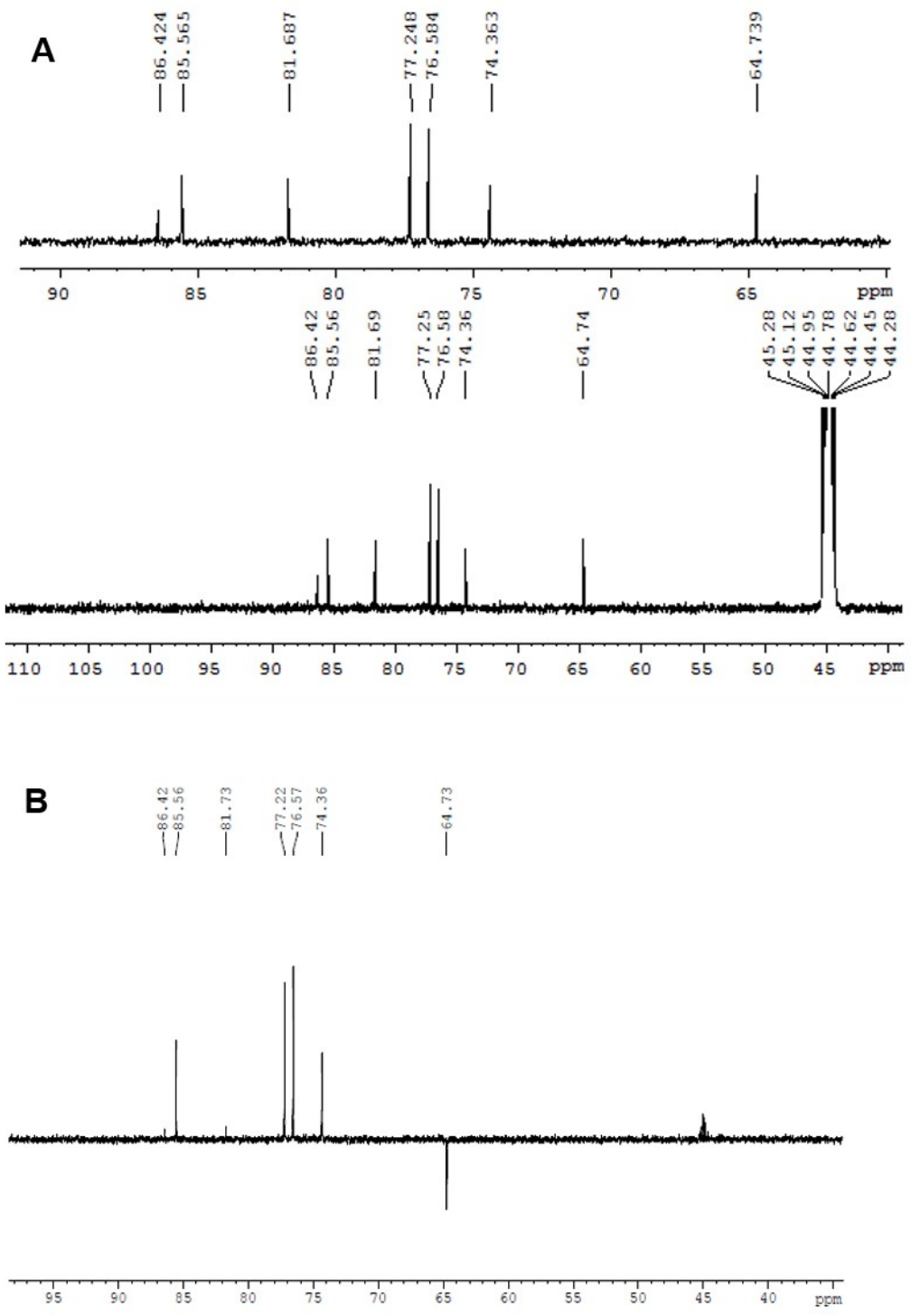

Figure S13. A) ^{13}C and B) DEPT135 spectra of monomer **1** in DMSO-d_6.

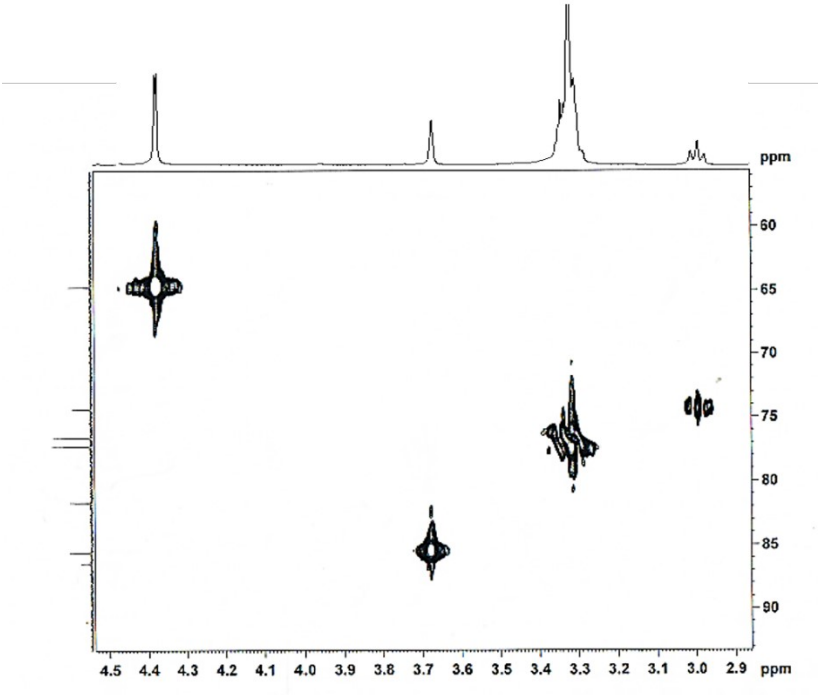

Figure S14. HMQC spectrum of monomer **1** in DMSO-d_6.

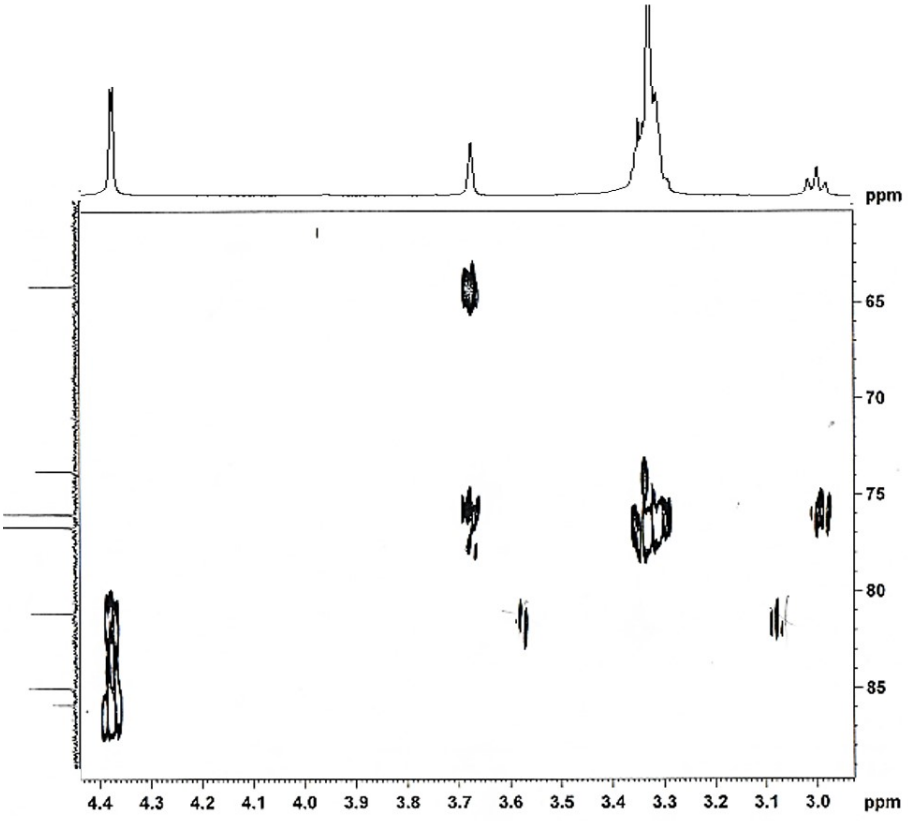

Figure S15. HMBC spectrum of monomer **1** in DMSO-d_6.

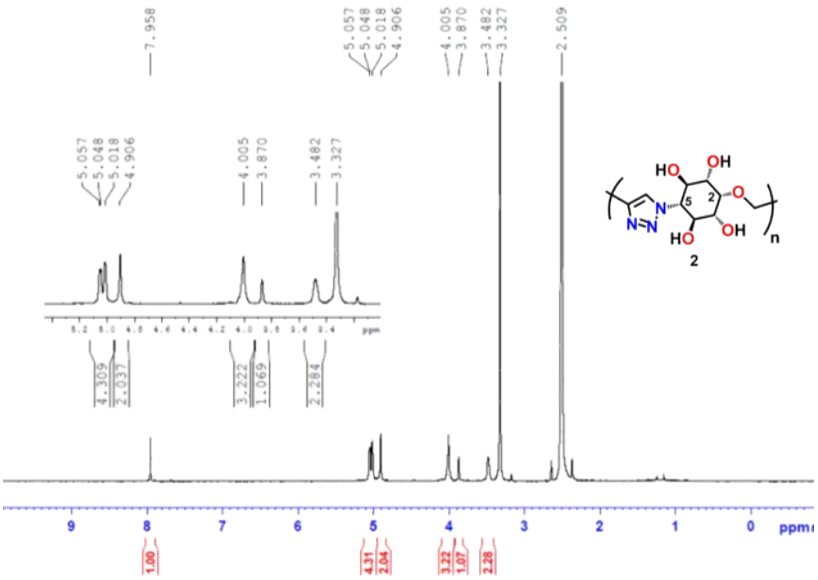

Figure S16. ^{1}H spectrum of polymer **2** in DMSO-d_6.

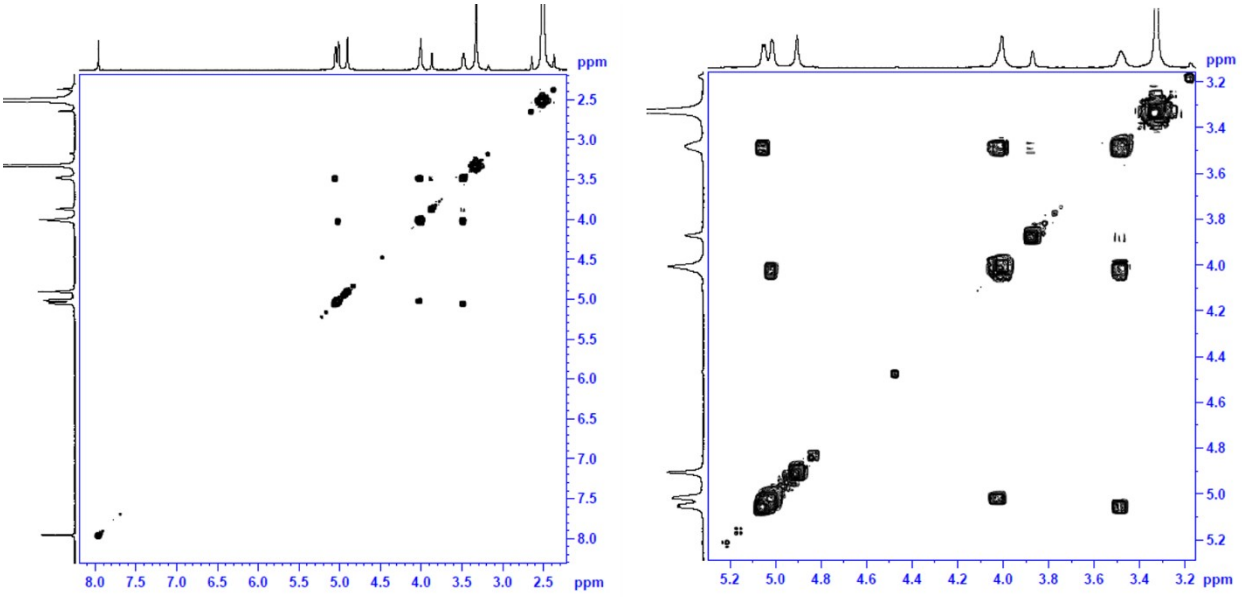

Figure S17. COSY spectrum of polymer **2** in DMSO-d_6.

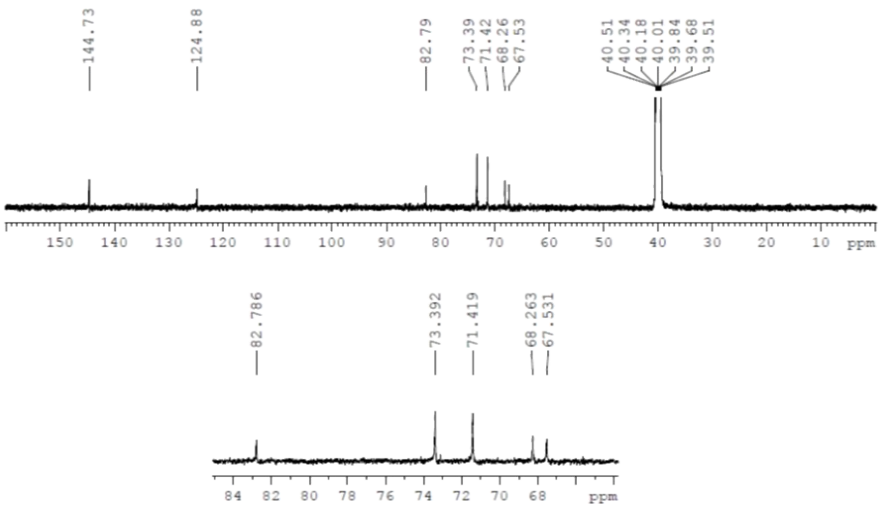

Figure S18. ^{13}C spectrum of polymer **2** in DMSO-d_6.

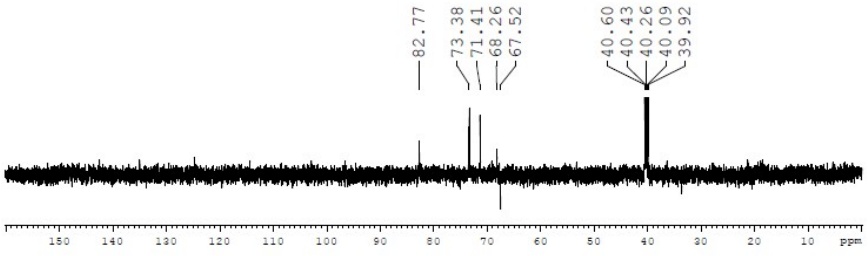

Figure S19. DEPT135 spectrum of polymer **2** in DMSO-d_6.

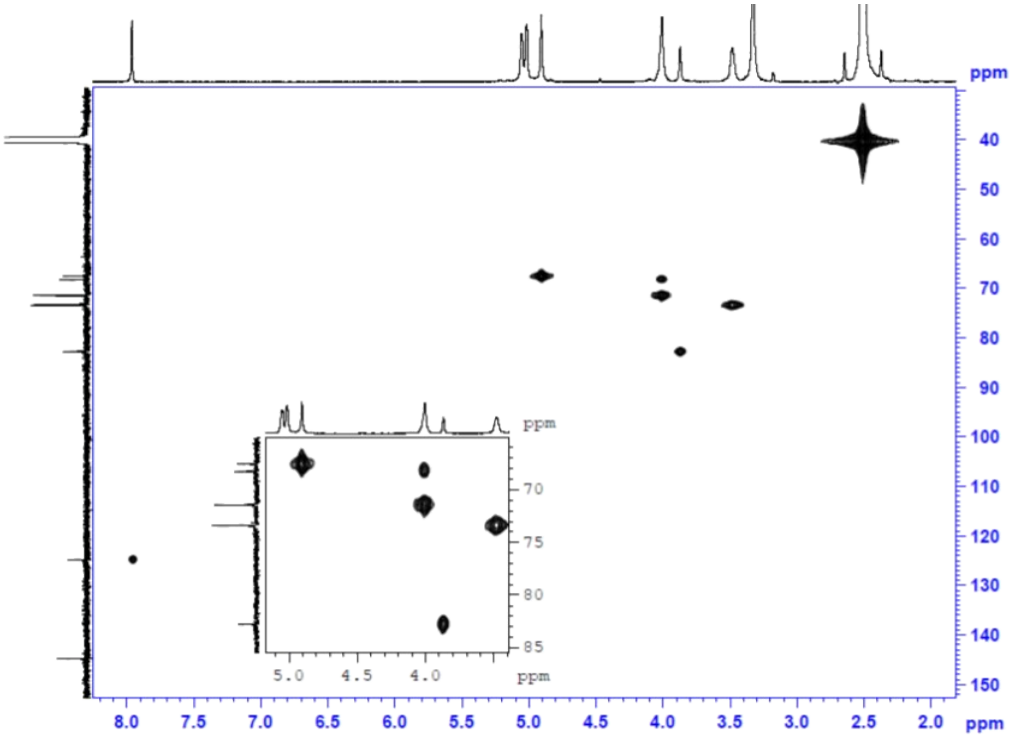

Figure S20. HMQC spectrum of polymer **2** in DMSO-d_6.

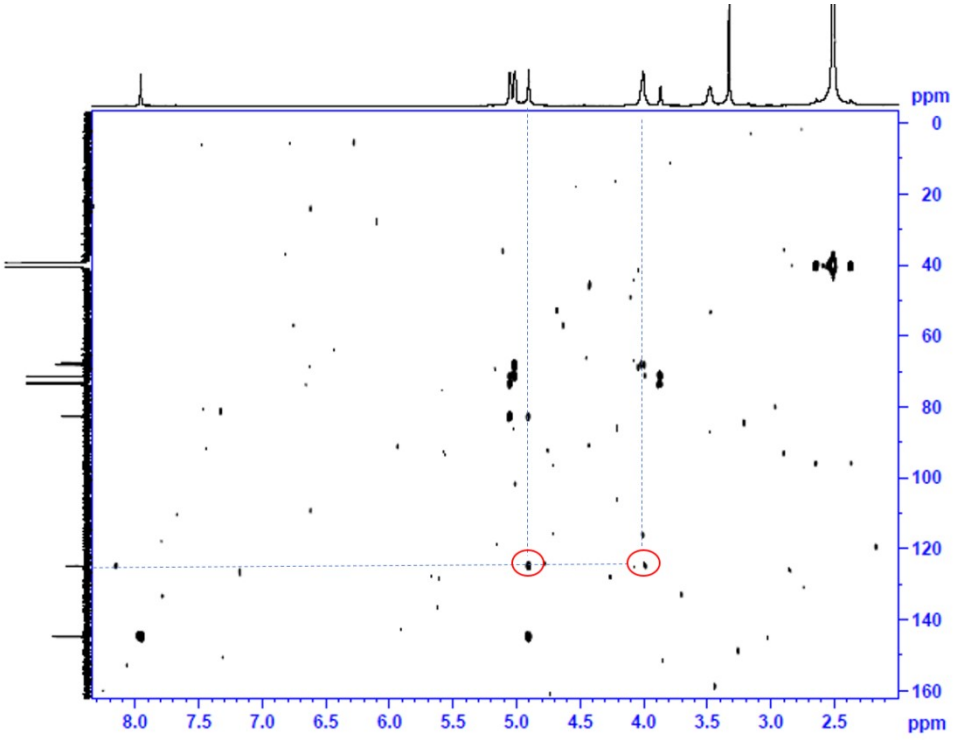

Figure S21. HMBC spectrum of polymer **2** in DMSO-d_6.

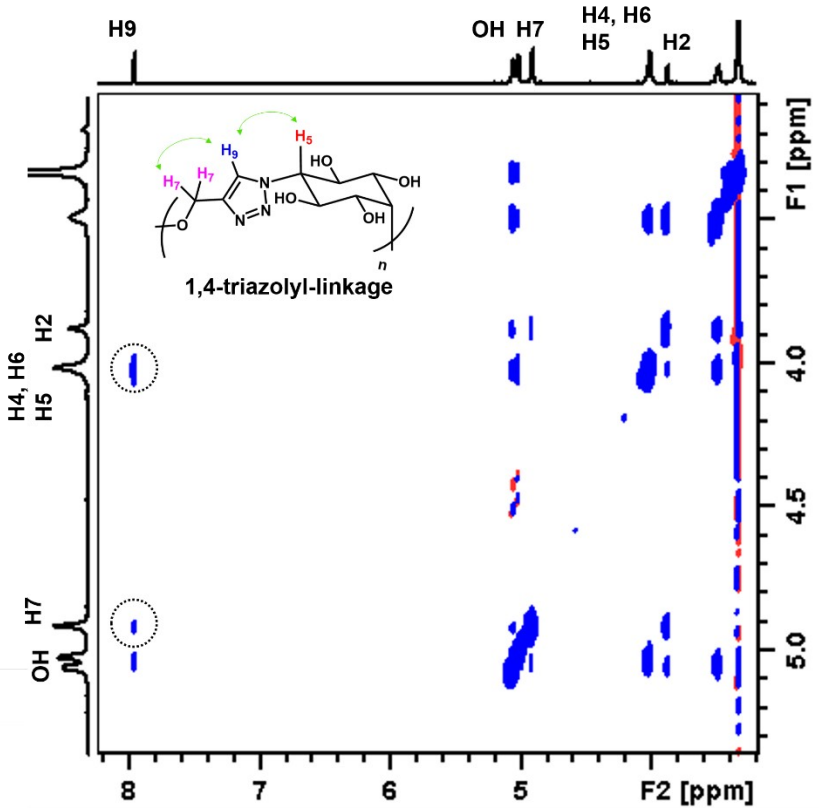

Figure S22. ^{1}H-^{1}H NOESY spectrum of polymer **2** in DMSO-d_6.

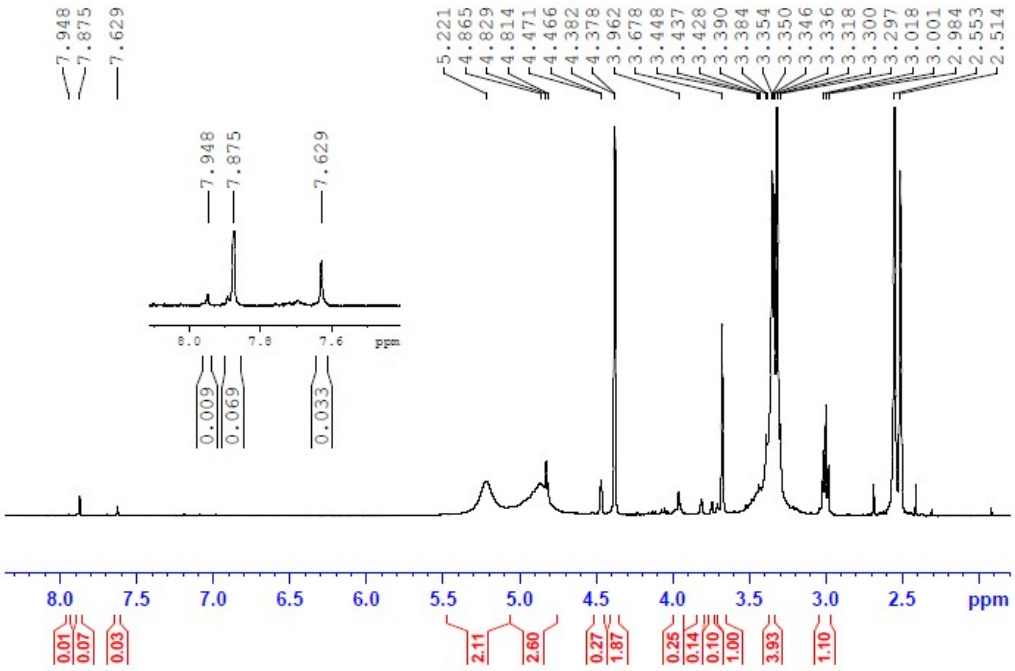

Figure S23. ^{1}H NMR spectrum of the monomer **1** heated to 100 ℃. The spectrum was recorded in DMSO-d_6.

13. References

[1] G. M. Sheldrick, *Acta Cryst.*, 2008, **D64**, 112-122.

[2] G. M. Sheldrick, *Acta Cryst.*, 2015, **C71**, 3-8.

[3] G. I. Birnbaum, *Can. J. Chem.*, 1977, **55**, 1619-1623.

[4] P. G. Jones, M. R. Edwards and A. J. Kirby, *Acta Cryst.*, 1989, **C45**, 244-247.

[5] A. K. Sah, C. P. Rao, P. K. Saarenketo, E. K. Wegelius, K. Rissanen and E. Kolehmainen, *J. Chem. Soc. Dalton Trans.*, 2000, 3681-3687.

[6] R. Luboradzki, O. Gronwald, M. Ikeda, S. Shinkai and D. N. Reinhoudt, *Tetrahedron*, 2000, **56**, 9595-9599.

[7] H.-R. Tang, P. S. Belton, S. C. Davies and D. L. Hughes, *Carbohydr. Res.*, 2001, **330**, 391-399.

[8] L. Jessen, E. T. K. Haupt and J. Heck, *Chem. Eur. J.*, 2001, **7**, 3791-3797.

[9] B. Bernet, R. Bürli, J. Xu and A. Vasella, *Helv. Chim. Acta*, 2002, **85**, 1800-1811.

[10] V. Lorbach, D. Franke, M. Nieger and M. Müller, *Chem. Commun.*, 2002, 494-495.

[11] G. Rajsekhar, U. B. Gangadharmath, C. P. Rao, P. Guionneau, P. K. Saarenketo and K. Rissanen, *Carbohydr. Res.*, 2002, **337**, 1477-1484.

[12] H. Wehlan, M. Dauber, M.-T. Mujica Fernaud, J. Schuppan, R. Mahrwald, B. Ziemer, M.-E. Juarez Garcia and U. Koert, *Angew. Chem. Int. Ed.*, 2004, **43**, 4597-4601.

[13] J. Hirsch, V. Langer and M. Koóš, *Molecules*, 2005, **10**, 251-258.

[14] A. Pathigoolla and K. M. Sureshan, *Angew. Chem. Int. Ed.*, 2013, **52**, 8671-8675.

[15] B. P. Krishnan and K. M. Sureshan, *ChemPhysChem*, 2016, **17**, 3062-3067.

[16] C. Wang, Q. Yan, Y. Wang, S. Huang, J. Ning, L. Feng, C. Sun, B. Zhang, D. Li and X. Ma, *J. Org. Chem.*, 2019, **84**, 1624-1629.

[17] A. Ravi and K. M. Sureshan, *Angew. Chem. Int. Ed.*, 2018, **57**, 9362-9366.